JASS 2008 - Joint Advanced Student School, Saint Petersburg, 9. - 19.3.2008
Modelling and Simulation in Multidisciplinary Engineering

Numerical Simulation of Noise Generation and Propagation In Turbomachinery

Seidl S.
Technische Universität München,
Lehrstuhl für Fluidmechanik – Abteilung Hydraulische Maschinen und Anlagen
D-85747 Garching Germany

Content

1 Introduction to Aeroacoustics
2 Lighthill's Analogy
3 Expansion about Incompressible Flow - An approach by Hardin & Pope
4 Numerical simulations
5 Conclusion
A Finite-Volume method
B Numerical methods for solving the hydrodynamic equations
C Linearisation of the conservation equations for acoustics

Technische Universität München
Fakultät für Maschinenbau

Lehrstuhl für Fluidmechanik · Abtlg. Hydr. Maschinen
o. Prof. Dr. Ing. habil. Rudolf Schilling

Numerical Simulation of Noise Generation and Propagation in Turbomachinery

Sascha Seidl

April 10, 2008

Contents

1 Introduction to Aeroacoustics **3**

2 Lighthill's analogy **5**

3 Expansion about Incompressible Flow - An approach by Hardin & Pope **9**

4 Numerical simulations **14**

5 Conclusion **23**

A Finite-Volume method **24**

B Numerical methods for solving the hydrodynamic equations **26**

C Linearisation of the conservation equations for acoustics **28**

1 Introduction to Aeroacoustics

The field of Aeroacoustics is that part of fluid dynamics, where the generation and propagation of sound in a moving medium are studied. Sound cannot be uniquely defined, therefore one definition is, that it represents density disturbances in the flow field. These disturbances propagate as waves over large distances through a medium, like liquids, gases or solids. Thus, sound is a change in pressure with respect to atmosphere, which can be perceived by the hearing sense of a human being. In contrast, noise is defined as unwanted sound.

Normally the sound waves generated by an unsteady flow process will only contain a small amount of the total power contained in the flow process. Therefore linear models for sound generation and propagation are possible in many cases.

Because of great differences in length and energy scales between the hydrodynamic and the acoustic field, a direct computation of the flow induced noise can only be realized by solving the complete compressible Navier-Stokes equations, which is done by a so called Direct Numerical Simulation. The great drawback of this DNS is the immense computational effort, as solving both the hydrodynamic and the acoustic field requires an extreme fine grid resolution. Thus, so called hybrid methods have been developed, which decouple the noise calculation into the computation of the flow field and the computation of the acoustic field.

The hybrid approach splits the computational domain into different regions, such that the governing flow or acoustic field can be solved independent with different equations and numerical techniques. This involves the usage of different numerical solvers, first a dedicated CFD tool and second an acoustic solver. The solution of the flow field is then used to calculate the acoustic sources. The computed acoustical sources are provided to the second solver which calculates the acoustical propagation. In this paper it will be distinguished between two approaches: the first one is an integral method based on the Lighthill analogy. The second method is the Expansion about Incompressible Flow technique, firstly formulated by Hardin & Pope and improved by Shen & Sørensen later on.

The classical model for sound generation is based on Lighthill's acoustic analogy and defines the sources of sound as the part of fluctuating density, that does not satisfy the classical wave equation. Lighthill's analogy is such a hybrid model and requires a priori knowledge about the unsteady flow field in order to calculate the sound sources. This approach will be pursued further in the second chapter.

In contrast to Lighthill's acoustic equation, Hardin & Pope reformulated the Navier-Stokes equations, achieving a nonlinear two-step procedure for computational aeroacoustics. This approach is suitable for both noise generation and propagation. First the viscous flow is obtained from the incompressible Navier-Stokes equations and a correction to the constant hydrodynamic density is defined. Afterwards a system of perturbed, compressible and inviscid equations is solved numerically, obtaining the acoustic radiation. Compared to the acoustic analogy theory, the splitting method has the advantage that the source strength is obtained directly and that it accounts for both sound radiation and scattering. The third chapter deals with the introduction of the hydrodynamic model, which is used to derive the new formulation of the Navier-Stokes equation as introduced by Hardin & Pope, subsequently resulting in the Expansion about Incompressible Flow method.

The last chapter illustrates several numerical simulations. As test cases two types of pumps are presented, a radial pump and an axial pump. For both pump types extensive experimental measurements for the hydrodynamic and acoustic behavior have already been performed. Therefore this data can be taken to validate the solutions from the numerical simulations made in chapter 4.

2 Lighthill's analogy

Lighthill reformulated the Navier-Stokes equations to derive a wave equation with a quadrupole-type source term, which includes a pressure and density contribution[1]. According to the Lighthill analogy, the noise due to an unsteady flow is equivalent to the noise that is generated by equivalent quadrupole sources radiating in a medium at rest. The quadrupole source strength is given by the Lighthill stress tensor.

Curle extended Lighthill's work in order to handle the influence of solid boundaries upon aerodynamic sound. Therefore Curle solved the Lighthill equation when the flow is interacting with a surface. According to Curle, the noise due to a flow passing by a body is equivalent to the noise that is generated by dipole sources on the surface of the body and quadrupole sources outside the surface. These dipole sources are given by the compressive stress tensor. The quadrupoles are given, as described above, by the vector velocity.

The third approach was made by Ffowcs-Williams and Hawkings, who extended the Lighthill and Curle models to take into account the interaction of the flow with rotating surfaces. To ensure that, they reformulated the Navier-Stokes equations introducing mathematical surfaces, that coincide with the surfaces of the moving solid, and imposing boundary conditions on it. According to their model the noise, as a result of flow interacting with the rotating surface, is due to three kinds of sources:

- **Monopoles**: thickness noise
- **Dipoles**: loading noise
- **Quadrupoles**: vortex noise.

Therefore the situation of an interacting flow with a rotating surface is equivalent to an acoustic medium at rest containing three source distributions:

$$\frac{\partial^2 \rho'}{\partial t^2} - a_s^2 \frac{\partial^2 \rho'}{\partial x_i^2} = \underbrace{\frac{\partial^2 \tau_{ij}}{\partial x_i \partial x_j}}_{(1)} - \underbrace{\frac{\partial f_i}{\partial x_i}}_{(2)} + \underbrace{\frac{\partial q}{\partial t}}_{(3)}, \tag{2.1}$$

containing the following quantities

- ρ' fluctuating density of the fluid,
- q specific alteration of the mass flow,

[1] Lilley showed that the quadrupole source term is more appropriately described by a dipole-type source term

- τ_{ij} stress tensor introduced by Lighthill,
- a_s speed of sound,
- f_i impressed specific force.

1. The first source term on the right hand side of (2.1) describes the **quadrupoles**, which represent the field distribution due to flow outside the surfaces, because of vortices and turbulence for example.

2. The second term stands for **dipoles**, which represent the surface distribution due to interaction of flow with moving bodies, as for example blade forces.

3. The last source term illustrates the **monopole** sources, which represent the surface distribution due to the volume displacement of fluid during the motion of the surfaces, because of rotating blades for example .

The derivation of Lighthill's acoustic equation will be presented below. As said before, Lighthill rearranged the Navier-Stokes equations, describing a flow of compressible viscous fluid to obtain an inhomogeneous wave equation.

First the continuity equation and the conservation of momentum equation are considered, which read

$$\frac{\partial \rho}{\partial t} + \frac{\partial (\rho u_i)}{\partial x_i} = 0, \tag{2.2}$$

$$\rho \frac{\partial u_i}{\partial t} + \rho u_j \frac{\partial u_i}{\partial x_j} = -\frac{\partial p}{\partial x_i} + f_i. \tag{2.3}$$

Multiplying the conservation of mass equation by u_i and adding the product to equation (2.3) gives

$$\frac{\partial (\rho u_i)}{\partial t} + \frac{\partial (\rho u_i u_j)}{\partial x_j} = -\frac{\partial p}{\partial x_i} + f_i. \tag{2.4}$$

Taking into account a source term q on the right hand side of the continuity equation, it becomes

$$\frac{\partial \rho}{\partial t} + \frac{\partial (\rho u_i)}{\partial x_i} = q. \tag{2.5}$$

Differentiating equation (2.5) with respect to time, and (2.4) with respect to x_i results in

$$\frac{\partial^2 \rho}{\partial t^2} + \frac{\partial^2 (\rho u_j)}{\partial t \partial x_j} = \frac{\partial q}{\partial t}, \tag{2.6}$$

$$\frac{\partial^2 (\rho u_i)}{\partial x_i \partial t} + \frac{\partial^2 (\rho u_i u_j)}{\partial x_i \partial x_j} = -\frac{\partial^2 p}{\partial x_i^2} + \frac{\partial f_i}{\partial x_i}. \tag{2.7}$$

By subtracting equation (2.7) from (2.6) one gets the acoustic wave equation, which reads

$$\frac{\partial^2 \rho}{\partial t^2} - \frac{\partial^2 p}{\partial x_i^2} = \frac{\partial q}{\partial t} - \frac{\partial f_i}{\partial x_i} + \frac{\partial^2}{\partial x_i \partial x_j}\Big(\rho u_i u_j\Big). \tag{2.8}$$

Linearisation of equation (2.8) by means of a perturbation ansatz gives

$$\rho = \rho_0 + \rho', \tag{2.9}$$

$$p = p_0 + p'. \tag{2.10}$$

Assume an isentropic state change, i.e.

$$\frac{\partial p}{\partial \rho} = \frac{\frac{\partial p}{\partial t}}{\frac{\partial \rho}{\partial t}} = a_s^2 = \gamma \cdot R \cdot T, \qquad \text{with} \tag{2.11}$$

- γ: heat capacity ratio
- **R**: gas constant
- **T**: temperature

Thus from equation (2.11) it follows by means of (2.9) and (2.10) that

$$\frac{\partial p'}{\partial \rho'} = a_s^2 = \gamma \cdot R \cdot T = \frac{\frac{\partial p'}{\partial t}}{\frac{\partial \rho'}{\partial t}}, \tag{2.12}$$

and with

$$\frac{\partial^2 \rho}{\partial t^2} = \frac{\partial^2 (\rho_0 + \rho')}{\partial t^2} = \frac{\partial^2 \rho'}{\partial t^2} = \frac{1}{a_s^2}\frac{\partial^2 p'}{\partial t^2}, \tag{2.13}$$

$$\frac{\partial^2 p}{\partial t^2} = \frac{\partial^2 (p_0 + p')}{\partial t^2} = \frac{\partial^2 p'}{\partial t^2}, \tag{2.14}$$

$$\frac{\partial}{\partial x_i \partial x_j}(\rho u_i u_j) = \frac{\partial}{\partial x_i \partial x_j}\Big(\rho_0 (U_i + u_i')(U_j + u_j')\Big), \tag{2.15}$$

where U_i is the time-dependent solution and u_i' the turbulence induced fluctuation velocity, one gets the acoustic wave equation for the alternating pressure $p'(x_i, t)$

$$\frac{1}{a_s^2}\frac{\partial^2 p'}{\partial t^2} - \frac{\partial^2 p'}{\partial x_i^2} = \frac{\partial q}{\partial t} - \frac{\partial f_i}{\partial x_i} + \frac{\partial^2}{\partial x_i \partial x_j}\Big(\rho_0 u_i u_j\Big). \tag{2.16}$$

Note that according to (2.13), the previous wave equation (2.16) is equivalent to the following expression

$$\frac{\partial^2 \rho'}{\partial t^2} - a_s^2 \frac{\partial^2 \rho'}{\partial x_i^2} = \frac{\partial q}{\partial t} - \frac{\partial f_i}{\partial x_i} + \frac{\partial^2}{\partial x_i \partial x_j}\Big(\rho_0 u_i u_j\Big). \tag{2.17}$$

Neglecting high order terms, the last term on the right hand side can be split into the spatial fluctuations of the temporal fluctuating momentum forces (a) and into the spatial fluctuations of the turbulent normal and shear stresses (b)

$$\begin{aligned}
\frac{\partial^2}{\partial x_i \partial x_j}\Big(\rho_0 u_i u_j\Big) &= \frac{\partial^2}{\partial x_i \partial x_j}\Big(\rho_0 U_i U_j\Big) + \frac{\partial^2}{\partial x_i \partial x_j}\Big(\rho_0 u_i' u_j'\Big) \\
&+ 2\left(\frac{\partial^2}{\partial x_1^2}\Big(\rho_0 U_1 u_1'\Big) + \frac{\partial^2}{\partial x_2^2}\Big(\rho_0 U_2 u_2'\Big)\right) \\
&+ \frac{\partial^2}{\partial x_1 \partial x_2}\Big(U_1 u_2' + U_2 u_1'\Big) \\
&= \underbrace{\frac{\partial^2}{\partial x_i \partial x_j}\Big(\rho_0 U_i U_j\Big)}_{(a)} - \underbrace{\frac{\partial^2}{\partial x_i \partial x_j}\Big[\underbrace{-\rho_0 u_i' u_j'}_{\equiv \tau_{ij}}\Big]}_{(b)} + \text{Mixed Terms.}
\end{aligned}$$

Note that Lighthill's equation is realized to be exact in that sense that no approximations of any kind have been made during its derivation.

3 Expansion about Incompressible Flow - An approach by Hardin & Pope

The hydrodynamic equations First of all consider a viscous compressible flow around a body. Let $\vec{u} = (u_1, u_2, u_3)$ denote the velocity vector, and ρ, p, T and S be the density, the static pressure, the temperature and the entropy per unit mass. Then the motion of fluid is governed by the compressible Navier-Stokes equations

$$\frac{\partial \rho}{\partial t} + \frac{\partial(\rho u_i)}{\partial x_i} = 0, \tag{3.1}$$

$$\frac{\partial(\rho u_i)}{\partial t} + \frac{\partial(\rho u_i u_j + p_{ij} - f_{viscous)}}{\partial x_j} = 0, \tag{3.2}$$

$$p = p(\rho, S), \tag{3.3}$$

$$\rho T \frac{DS}{Dt} = \rho c_p \frac{DT}{Dt} - \beta T \frac{Dp}{Dt} = \rho\phi + \frac{\partial}{\partial x_i}\left(k \frac{\partial T}{\partial x_i}\right), \tag{3.4}$$

where c_p, β and k are the specific heat capacity at constant pressure, the coefficient of thermal expansion and the coefficient of thermal conductivity. Respectively, ϕ denotes the viscous dissipation. The coefficient of thermal expansion is defined by

$$\beta = -\frac{1}{\rho}\left(\frac{\partial \rho}{\partial T}\right)_p.$$

Note that

$$\frac{D}{Dt} = \frac{\partial}{\partial t} + (u.\triangle)$$

Furthermore there is

$$p_{ij} = p\delta_{ij} - \mu\left[\frac{\partial u_i}{\partial x_j} + \frac{\partial u_j}{\partial x_i} - \frac{2}{3}\left(\frac{\partial u_k}{\partial x_k}\right)\right],$$

where μ is the dynamic viscosity.

The investigations shall be restricted to the case of $Ma \leq 0.3$. Thus we employ an incompressible flow solver, and therefore we can set $Ma = 0$. The incompressible solution can be obtained by the incompressible Navier-Stokes equations, which read in primitive variables

$$\frac{\partial U_i}{\partial x_i} = 0, \tag{3.5}$$

$$\frac{\partial U_i}{\partial t} + \frac{\partial(U_i U_j)}{\partial x_j} = -\frac{1}{\rho_0}\frac{\partial P}{\partial x_i} + \nu \frac{\partial^2 U_i}{\partial x_j^2}. \tag{3.6}$$

where P, ρ_0 and U_i are the incompressible pressure, the ambient density and the velocity components.

The pressure change from ambient pressure p_0 is given by

$$dp = P - p_0. \tag{3.7}$$

Although these changes are computed under the assumption of constant density, no fluid is truly incompressible. Thus equation (3.3) implies

$$dp = \left(\frac{\partial p}{\partial \rho}\right)_S d\rho + \left(\frac{\partial p}{\partial S}\right)_\rho dS = a_s^2 d\rho + \left(\frac{\partial p}{\partial S}\right)_\rho dS, \tag{3.8}$$

where the speed of sound is defined as

$$a_s = \sqrt{\left(\frac{\partial p}{\partial \rho}\right)_S}.$$

The preceding equation (3.8) is usually solved along with (3.4), and indicates that the pressure change is associated with density and entropy changes at the same time if the speed of sound takes a value unequal to infinity. According to this, the incompressible pressure is dependent on ρ and S. It is noted that after [Shen&Sørensen99b], little generality is lost by assuming the flow to be isentropic, as the pressure distribution is rather modified by the effects of viscosity and heat conduction than that the magnitude of pressure variation is controlled by them. That means that these effects are slow on an acoustic time-scale. By introducing the time-averaged incompressible pressure distribution

$$\bar{P}(x) = \lim_{T\to\infty} \frac{1}{T} \int_0^T P(x,t)dt,$$

an isentropic[2] pressure fluctuation in time $p - \bar{P}$ can be assumed, and the entropy changes only for the averaged pressure $\bar{P}$. Thus the pressure term can be decomposed by

$$p(\rho, S) = p^*(\rho) + \bar{P}(S). \tag{3.9}$$

Only the averaged incompressible pressure $\bar{P}$ involves losses, whereas the pressure fluctuation p^* is assumed to be isentropic. Derivation of equation (3.9) with respect to time gives

$$\frac{\partial p}{\partial t} = \frac{\partial p^*}{\partial t} = \frac{dp^*}{d\rho}\frac{\partial \rho}{\partial t} = \left(\frac{\partial p}{\partial \rho}\right)_S \frac{\partial \rho}{\partial t} = a_s^2 \frac{\partial \rho}{\partial t}, \qquad \text{with } a_s = a_s(x). \tag{3.10}$$

This implies that there is no need for an energy equation (3.4) in acoustics description.

[2] at constant entropy

Expansion about Incompressible Flow Using a numerical mesh with an adequate fine resolution the exact numerical solution of the Navier-Stokes equations provides both the fluiddynamic and acoustic quantities within the same solution vector

$$\begin{bmatrix} \rho(x_i,t) \\ u_i(x_i,t) \\ p(x_i,t) \end{bmatrix}.$$

The direct computation of the Navier-Stokes equations in combination with the appropriate state equations yet demands a grid size for a three-dimensional unsteady flow, whose number of mesh points N is proportional to the third power of the Reynolds number

$$N \sim Re^3.$$

Therefore for technically interesting flows with a Reynolds number $Re > 10^5$ an immense number of mesh points has to be used to describe the fluiddynamic as well as the acoustic characteristics of the flow field.

As the acoustic fluctuations are considerably smaller than the fluiddynamic variables as a result of turbulence, Hardin & Pope proposed a separation of fluiddynamic and acoustic quantities by means of a perturbation approach.

Consider the compressible Navier-Stokes equations given by (3.1) till (3.4). Hardin & Pope proposed a nonlinear two-step procedure for computational aeroacoustics which is suitable for both noise generation and propagation (see [Hardin&Pope94]). This approach is called Expansion about Incompressible Flow and splits the flow field with methods of flow computation into an incompressible viscous flow field and a compressible inviscid acoustic field. Thus the viscous flow is obtained from the incompressible Navier-Stokes equations. Using a correction to the constant hydrodynamic density, the acoustic radiation is obtained from the numerical solution of a system of perturbed, compressible and inviscid equations. Note that the EIF is only possible under the following assumption: The generation and propagation of noise is influenced by the motion of the fluid, conversely there exists no retroactivity from the acoustic field on the hydrodynamic flow field.

Since the approach after Hardin & Pope is only suitable for isentropic flows, Shen & Sørensen reformulated the model, which can be applied now on both isentropic and non-isentropic flows (see [Shen&Sørensen99b]).

First, the following decomposition for the compressible solution is used

$$\begin{array}{ccccc} u_i(x_i,t) & = & U_i(x_i,t) & + & u_i'(x_i,t) \\ p(x_i,t) & = & P(x_i,t) & + & p'(x_i,t) \\ \rho(x_i,t) & = & \rho_0(x_i,t) & + & \rho'(x_i,t) \end{array}$$

Exact numerical solution of the fluiddynamic and acoustic problem	Unsteady flow variables without acoustic portion	Acoustic quantities, sound propagation

where u_i' and p' are the fluctuations of the velocity components and pressure about their incompressible counterparts and the variable ρ' is the fluctuating density about ρ_0. Note that for incompressible fluids or flows of a compressible fluid with Mach number $Ma < 0.3$ it can be set $\rho_0 = \text{const}$.

Next, an acoustic variable f is introduced

$$f_i = \rho \cdot u_i' + U_i \cdot \rho', \qquad \text{and } \rho = \rho_0 + \rho'. \tag{3.11}$$

Inserting the decomposition equations from above into the hydrodynamic equations (3.1) and (3.2) plus equation (3.10) and neglecting terms of viscosity on the fluctuations, the following first-oder nonlinear formulation of the acoustic equations for computation of the perturbation quantities is obtained

$$\frac{\partial \rho'}{\partial t} + \frac{\partial f_i}{\partial x_i} = 0, \tag{3.12}$$

$$\frac{\partial f_i}{\partial t} + \frac{\partial}{\partial x_j}\Big[f_i(U_j + u_j') + \rho_0 U_i u_j' + p'\delta_{ij}\Big] = 0, \tag{3.13}$$

$$\frac{\partial p'}{\partial t} - a_s^2 \frac{\partial \rho'}{\partial t} = -\frac{\partial P}{\partial t} \tag{3.14}$$

The speed of sound is given by

$$a_s^2 = \gamma \cdot \frac{p}{\rho} = \gamma \frac{P + p'}{\rho_0 + \rho'}, \qquad \text{with } \gamma = \frac{c_p}{c_v} = 1.4$$

Reshaping equation (3.14) by means of (3.12), one gets

$$\frac{\partial p'}{\partial t} + a_s^2 \frac{\partial f_i}{\partial x_i} = -\frac{\partial P}{\partial t}. \tag{3.15}$$

It shall be noted that there is only one single acoustic source coming from the incompressible solution which is the instantaneous pressure. Therefore the acoustic calculation can be started at any time during the incompressible computation.

The acoustic variable f_i can be computed from the momentum conservation equation (3.13), the density fluctuation ρ' from the continuity equation (3.12), the velocity fluctuations from the definition of the acoustic variable (3.11) and the pressure fluctuation p' is determined by the isentropic relation equation (3.14) for the density and pressure fluctuations.

Thus the acoustic quantities can be calculated directly from the previously computed solution of the flow field $\{u_i'(x_i,t), p'(x_i,t)\}$, that means from the temporal variation of the pressure field $P(t)$, the spatial distribution of the velocity $U_i(x_i)$ and the turbulence of the stream.

Initial and boundary conditions For completion of the numerical model the initial and boundary conditions are still missing.

The appropriate initial conditions at the inlet are given as follows

$$\begin{aligned} \rho' &= 0, \\ u_i' &= 0 \quad \text{respectively } f_i = 0, \\ p' &= p_0 - P, \end{aligned}$$

where p_0 denotes the constant ambient pressure.

As the equations (3.12) till (3.14) are inviscid, the only boundary condition at solid walls is the slip condition $u_n = 0$, so for the variable f it is $f_n = 0$ ($u_n \equiv 0 \equiv f_n$).

At the far field of the computational domain, acoustic boundary conditions have been proposed by Tam and Webb, using cylindrical coordinates (see [Tam&Webb93]). The following radiation boundary conditions are used at those boundaries, where there are only outgoing acoustic waves

$$\begin{aligned} \frac{\partial \rho'}{\partial t} + (u_n + a_s)\left(\frac{\partial \rho'}{\partial r} + \frac{1}{2}\frac{\rho'}{r}\right) &= 0, \\ \frac{\partial u_i'}{\partial t} + (u_n + a_s)\left(\frac{\partial u_i'}{\partial r} + \frac{1}{2}\frac{u_i'}{r}\right) &= 0, \\ \frac{\partial p'}{\partial t} + (u_n + a_s)\left(\frac{\partial p'}{\partial r} + \frac{1}{2}\frac{p'}{r}\right) &= 0. \end{aligned}$$

These boundaries are non-reflecting boundaries, reducing non-physical reflection from computational boundaries.

4 Numerical simulations

The simulation of sound generation and propagation will be realized by a commercial tool called SYSNOISE, which is based on the aeroacoustic analogy after Lighthill. The acoustic sources are defined, following the solution of the flow simulation. Therefore the transient solutions for pressure and velocity, that are part of the instationary flow solution, are transmitted by an interface from the hydrodynamic solver NS3D to the acoustic program SYSNOISE. The tool NS3D has been developed at the Institute of Fluid Mechanics of the TUM and is based on a Finite-Volume scheme.

In the following two test cases will be presented:

- Radial pump RP28
- Axial pump AP149

Investigation of the radial pump The radial pump is provided by the company WILO AG, which already performed flow and acoustic measurements for validation. It has an impeller with seven blades and a characteristic Reynolds number of $Re = 6 \cdot 10^5$. The radial pump will be analyzed at the following operating points:

- **Optimal load**: $Q = 2.5\frac{m^3}{h},\ n = 2524\frac{1}{min}$
- **Partial load**: $Q = 1.0\frac{m^3}{h},\ n = 2690\frac{1}{min}$

With respect to the high computational time, which is necessary for a comparable simulation, a grid with $N = 1.30 \cdot 10^6$ grid points was attached, as can be seen in Fig.3.

The greatest pressure fluctuations appear near the tongue in the pump spiral case, which is shown in Fig.4. Therefore the investigations will be restricted to that point of the pump.

The computation of the sound radiation occurs by means of a direct BEM[3] calculation. On the one side the sound sources are defined by rotating dipoles on the surface of the blades, as well as there are distributed fixed dipole sources on the surface in the outlet area. The surface grid for the BEM calculation for the sound generation, which is shown in Fig.5, includes 4918 triangles and quads with 4827 nodes in total.

In a first approach, the sound generation resulting from pressure fluctuations at the rotating blades was investigated. It could be shown that the resulting sound at the outlet of

[3]Boundary Element Method: Boundary oriented discretization method, i.e. it uses only a grid at the edge of the computational domain neglecting any grid points from inside.

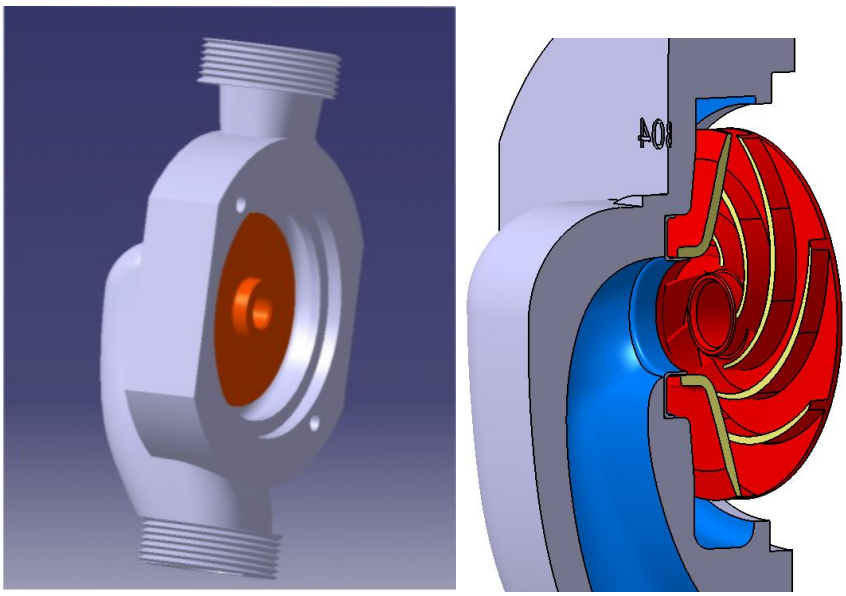

Figure 1: Geometry of the radial pump RP28

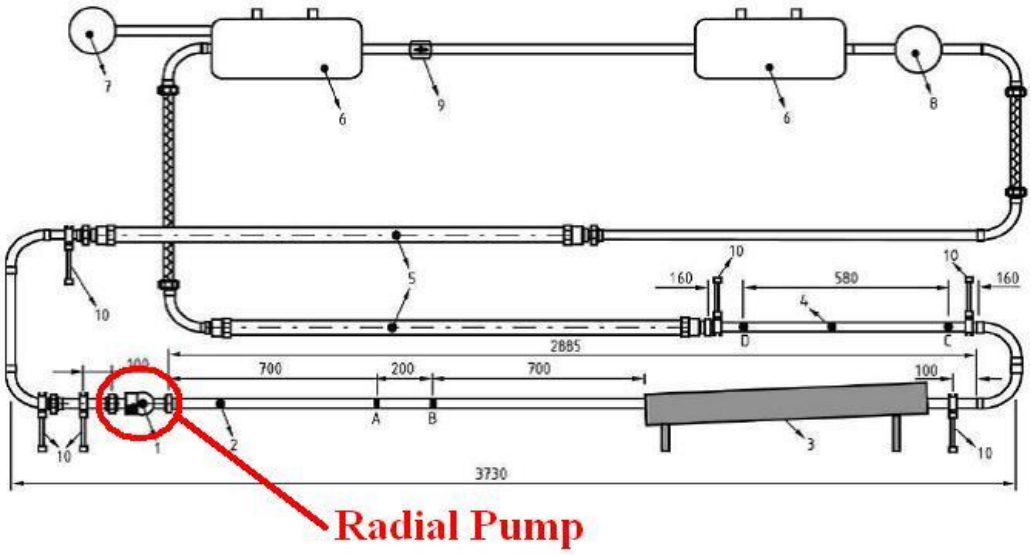

Figure 2: The complete installation with the radial pump

the pump was too small. Therefore additional pressure fluctuations in the interior of the pump were considered. In a second step the area around the outlet had been involved as alternative sound source, thus defining fixed dipoles in the tongue area. Fig.6a and Fig.6b show the trace of either the rotating dipoles and the area of the fixed dipole sources at the tongue.

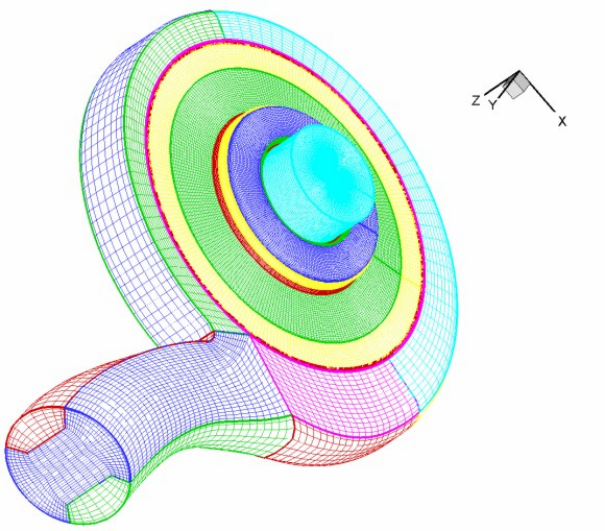

Figure 3: Computational grid for impeller and the spiral case

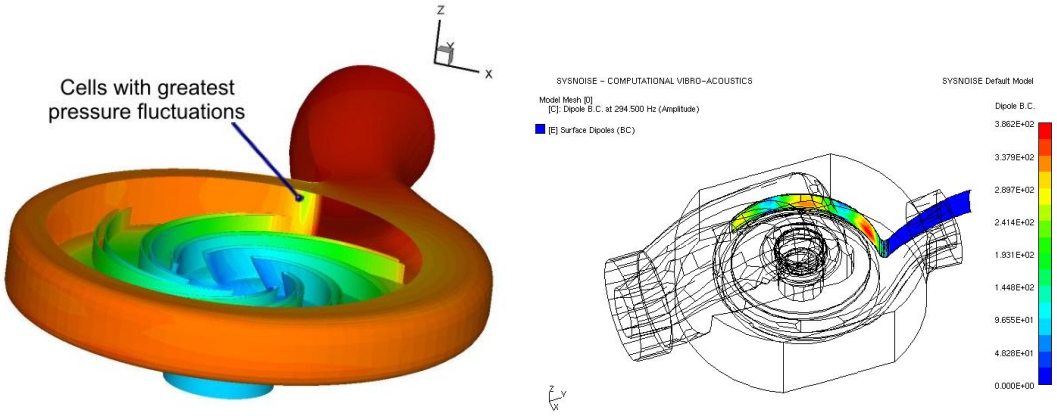

Figure 4: Pressure fluctuations in the pump

A first comparison between the computed results shows, that the influence of the rotating sound sources on the blades can be neglected compared to the sound sources situated at the tongue. In Fig.7 the results of the computation for the fixed dipoles, as well as the measurements made by WILO AG for the operating point under optimal load with flowrate $Q = 2.5\ \frac{m^3}{h}$ are plotted. Whereas Fig.8 shows the results attained under partial load $Q = 1.0\ \frac{m^3}{h}$. The results for the influence of the rotating dipoles for both operating points are presented in Fig.9. By comparing the computed flow-induced sound power resulting on the one side from the fixed dipoles, and on the other side from the rotating dipoles, one notes that the influence of the rotating dipoles in contrast to the fixed ones can be neglected. Therefore the focus of further investigations lies on the areas of distributed fixed dipoles.

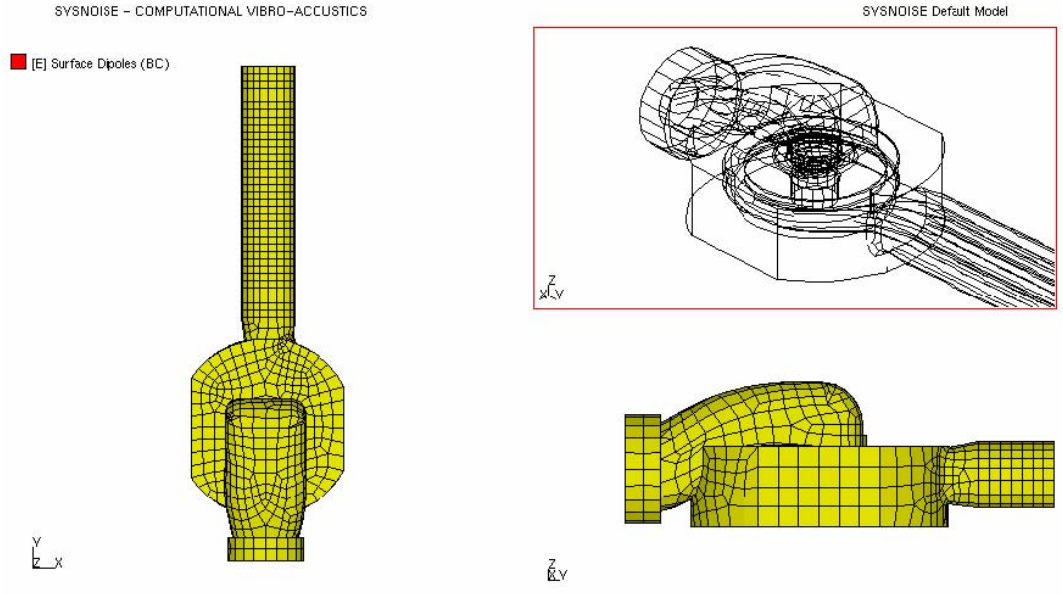

Figure 5: Computational grid for acoustic computations

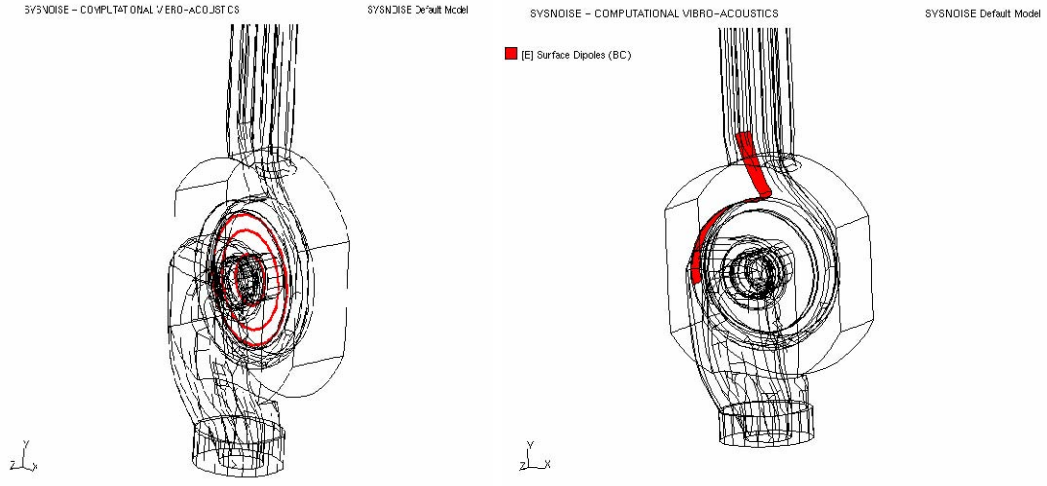

Figure 6: Definition of the (LEFT) rotating dipole sources and (RIGHT) fixed dipole sources at the tongue

Moreover, the dominating sound sources appear not only on the blades, but rather at the outlet area. Thus, continuative evaluation will only take place for fixed dipoles on the surfaces of the pump body. The emphasized fields shown in Fig.10 contain the field of greatest pressure fluctuations in the interior of the pump. Fig.10b also includes additional faces for the definition of further source terms in the hydrodynamic equations.

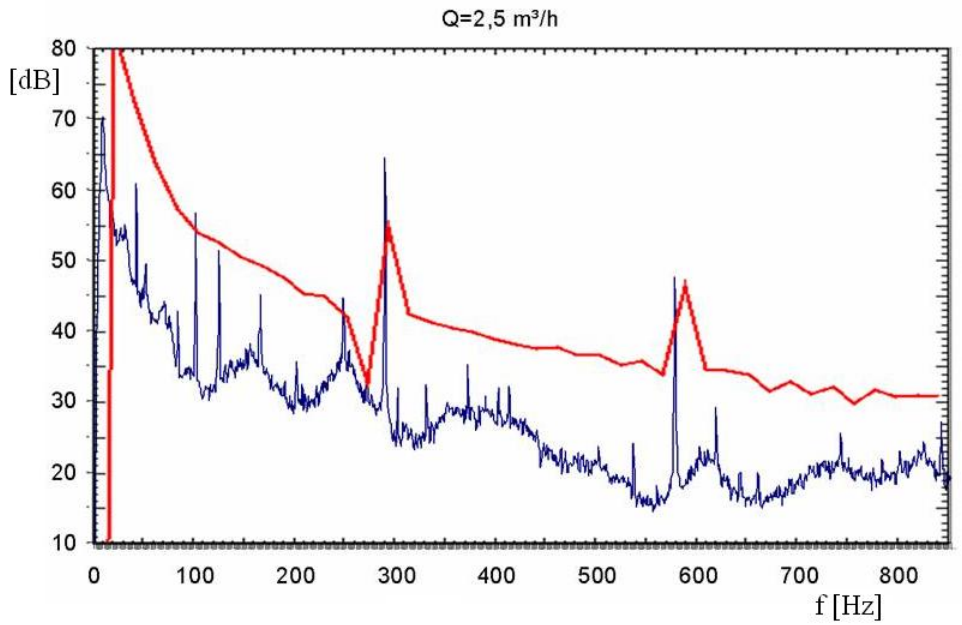

Figure 7: Flow-induced sound power through fixed dipoles under optimal load $Q = 2.5\ \frac{m^3}{h}$; blue measurement, red computation

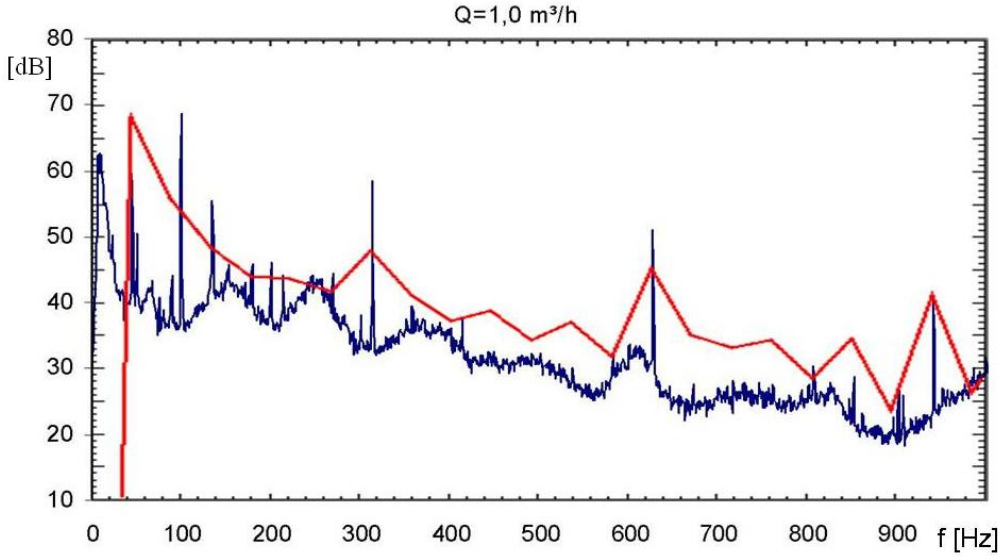

Figure 8: Flow-induced sound power through fixed dipoles under partial load $Q = 1.0\ \frac{m^3}{h}$; blue measurement, red computation

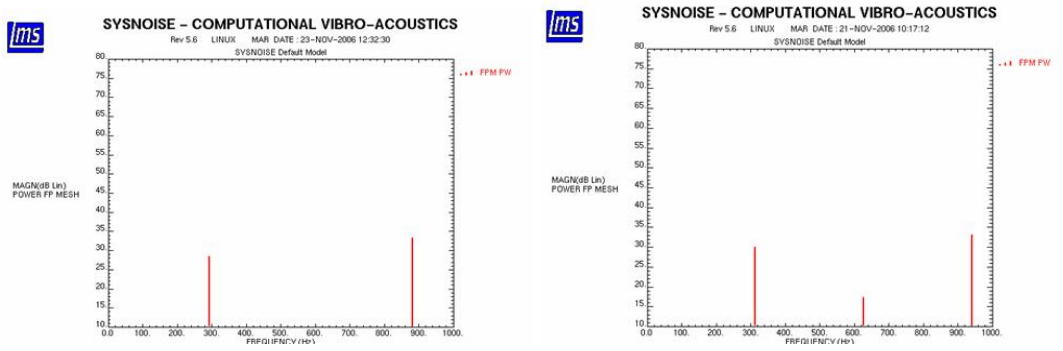

Figure 9: Flow-induced sound power through rotating dipoles under partial load; (LEFT) $Q = 2.5\ \frac{m^3}{h}$, (RIGHT) $Q = 1.0\ \frac{m^3}{h}$

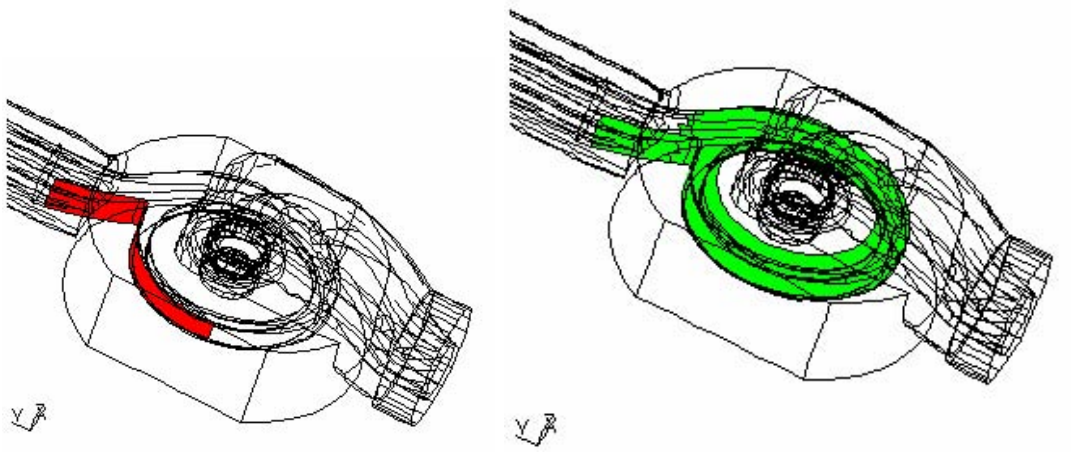

Figure 10: Definition of the distributed dipoles a) nose area and b) extended area

The solution for the computed flow-induced acoustic power at the outlet under optimal load is shown in Fig.11, the results under partial load are shown in Fig.12. Comparison of the two results shows clearly that the dominating dipole sources are situated at the tongue of the pump. Consideration of additional dipole sources in the extended area has nearly no influence on the computed acoustic power, as can be seen from the matching lines b) and c) in Fig.11 and Fig.12.

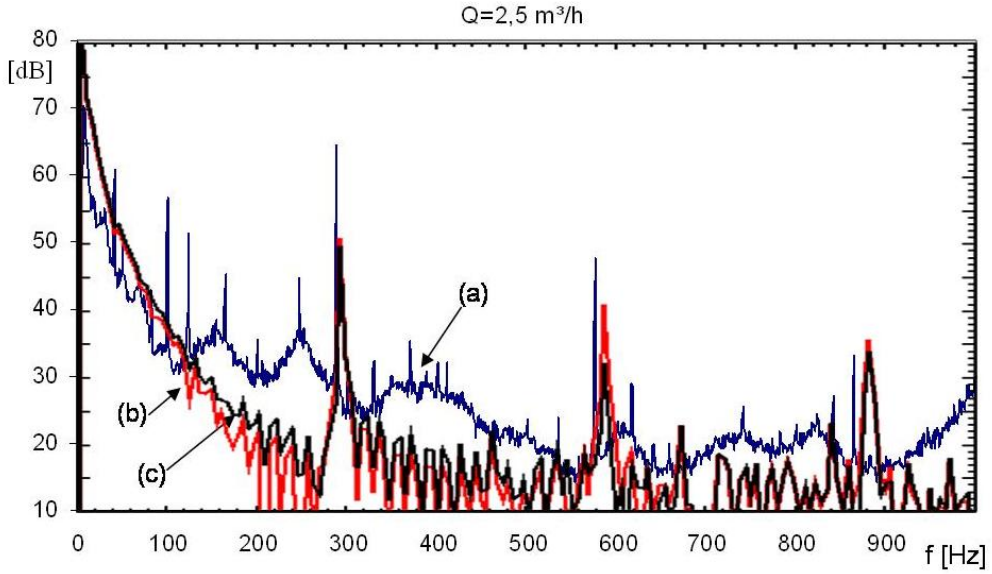

Figure 11: Flow-induced acoustic power under optimal load (a) measurement (b) calculation with dipoles in the tongue area (c) calculation with dipoles in the extended area

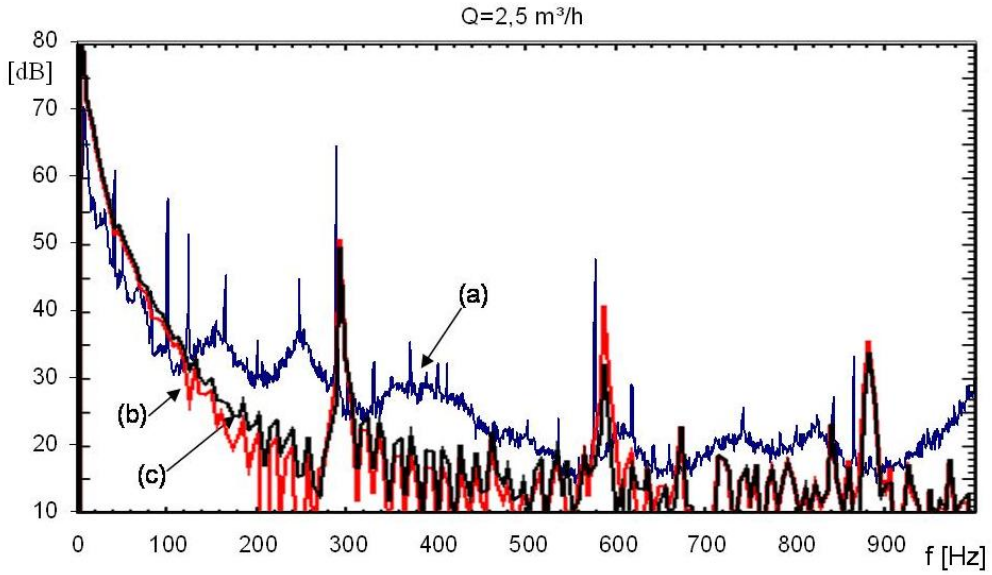

Figure 12: Flow-induced acoustic power under partial load (a) measurement (b) calculation with dipoles in the tongue area (c) calculation with dipoles in the extended area

Axial Pump AP149 The considered axial flow pump has a specific rotational frequency of $n_q \approx 150$ and its rotor consists of $Z_{rot} = 16$ blades, whereas its stator features $Z_{stat} = 19$ blades. For validation purposes, investigations at the TU Braunschweig had been made beforehand.

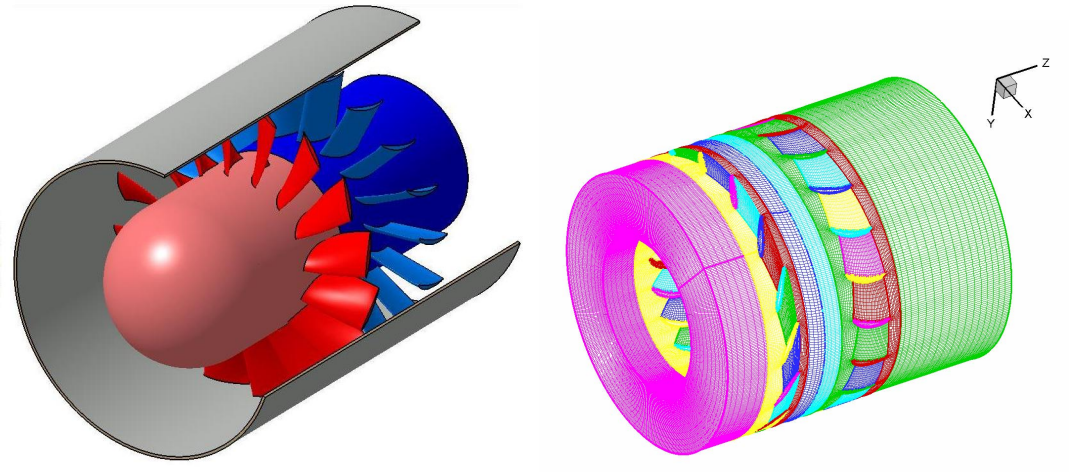

Figure 13: Geometry and meshing of the axial pump

Adopting the same procedure as in the case of the radial pump, the hydrodynamic equations will be solved first. Afterwards the acoustic problem will be considered with the hydrodynamic quantities determined before. Therefore the blading of the rotor will be discretized with $N_{rot} = 321832$ grid points, and the stator with $N_{stat} = 508130$ grid points.

Analyzing the hydrodynamic flow field, it can be seen that the most intense pressure fluctuations arise at the hub, where rotor-stator interaction takes place, more exactly, where the unsteady rotor flow hits the tip of the stator.

The computation of the acoustic field is based on the results of the flow solution. As said above, the greatest pressure fluctuations appear at the front side of the stator blades. Therefore we consider only fixed dipoles at the stator as acoustic sources. In Fig.14 the temporal distribution of the flow solution at a characteristic point is shown.

The surface mesh for the acoustic computation by means of BEM consists of about 4500 elements with almost 4500 nodes. The calculation of the sound radiation by means of direct BEM results from coupling the interior problem with the exterior problem, that means the dipoles on the stator blades are evaluated in order to calculate the noise levels on the in- and outlet surfaces. The analysis of the pump is performed over a frequency

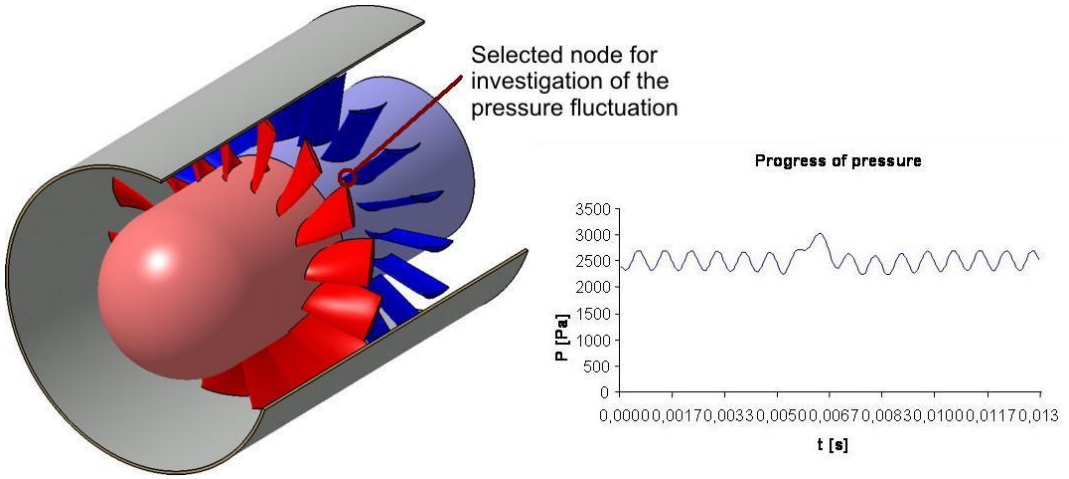

Figure 14: Temporal alteration of the pressure for one rotation in one point at the front of one stator blade

domain up to 1500 Hz with frequency steps of $\triangle f = 75$ Hz. Fig.15 shows the acoustic power for a spherical field-point-area with distance 2 m to the origin of the pump. We can see clearly the maximal characteristic frequency at 1200 Hz.

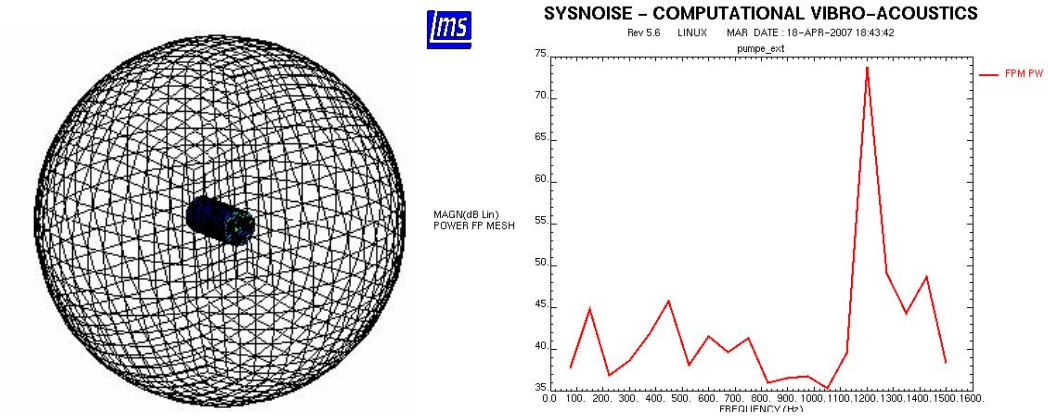

Figure 15: Field-point-area and acoustic power radiated from the axial pump

5 Conclusion

Two models for the generation and propagation of noise induced by fluid motion through a turbo machinery have been introduced and described. Although there are only test cases for the Lighthill analogy available, as the EIF approach has not been implemented in the NS3D code and tested yet, the method after Lighthill in its original form is not suitable for solving the acoustic problem strictly speaking, as the theory presumes an unresisted sound propagation. For more complex geometries like in channels, turbines or pumps, where the fluid flow and subsequent the sound propagation is restricted to solid walls, the Lighthill analogy fails, as it acts on the assumption of an unbounded computational domain. Therefore sound radiation is modeled only into free space. Effects of reflexion, absorption or refraction by solid boundaries can only be considered by using additional methods, like the BEM etc.

The numerical simulations show exactly the just described issues: Because of the simplified modeling after Lighthill the acoustic power level is computed improperly, as the sound radiation from the body of the pump is computed inadequately and the sound passing through its body is not computed at all.

In contrast the approach after Hardin & Pope does not get influenced by those limitations described above. Furthermore it is generally accepted in the context of small density fluctuations. Another great advantage over Lighthill's equation is the possibility, due to the splitting of viscous and acoustic problems, to adapt one grid system and integration scheme for the solution of the viscous incompressible equations, while a completely different grid and integration scheme can be designed for the solution of the acoustic perturbations. Moreover it is supposed that the EIF produces more exact predictions of the noise generation and propagation than Lighthill does. Therefore the investigations to the acoustic problem shall be pursued by using the Expansion about Incompressible Flow approach.

A Finite-Volume method

The FVM subdivides the solution domain into a finite number of small control volumes. These are organized on a grid, which defines the control volume boundaries. For every control volume the required equations are approximated, resulting in a balance equation for each cell. Those balance equations produce relations between the conservative quantities and the in- and outgoing flows over the cell boundaries as well as the sources and drains present in the cells. The control volumes are built in the following order: the cell center is named P, the centers of the cell neighbors are referred to as N, S, W, E, B, T. Two neighboring cells have a joint cell face with the surface area F.

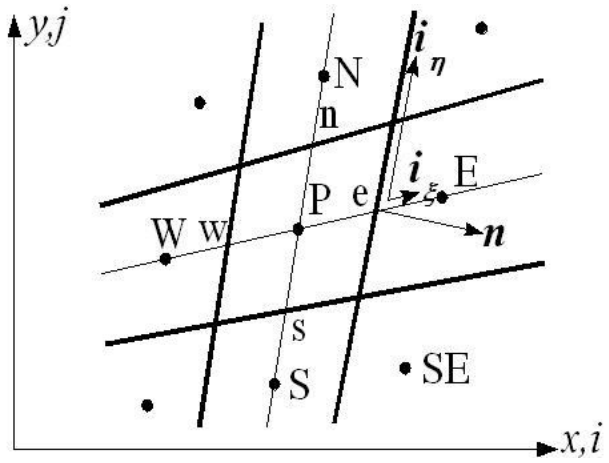

Figure 16: Control volumes for the 2D case

We describe the discretization of the general transport equation, which models the transportation of a general quantity Φ. For the numerical simulation the transport equation is integrated over the volume of the computational domain, i.e.

$$\int_\Omega \left(\frac{\partial \Phi}{\partial t}\right) d\Omega + \int_\Omega \left(\frac{\partial (u_j \Phi)}{\partial x_j}\right) d\Omega = \int_\Omega \left(\frac{\partial}{\partial x_i}\left(\Gamma \frac{\partial \Phi}{\partial x_j}\right)\right) d\Omega + \int_\Omega q_\Phi d\Omega.$$

On the right hand side of the preceding equation, Γ denotes the diffusion coefficient, and q_Φ the source term. By using the divergence theorem after Gauß the volume integrals of the convective and diffusive terms can be transformed to surface integrals

$$\frac{\partial}{\partial t}\int_\Omega \Phi d\Omega + \int_S \Phi u_j \mathbf{n}_j dS = \int_S \Gamma \frac{\partial \Phi}{\partial x_j}\mathbf{n}_j dS + \int_\Omega q_\Phi d\Omega.$$

The evaluation of the surface integrals has to be done for each cell face and follows the same procedure for each face.

Approximation of surface integrals To calculate the integral over a surface the distribution of the flow f over the face must be known. The term is distinguished between $f^c = \Phi u_j \mathbf{n}_j$ and $f^d = \Gamma(\partial\Phi/\partial x_j)\mathbf{n}_j$. Therefore we have to split the total face in either four or six cell faces, for 2 or 3 dimensions respectively. With the integral flow $F_l \approx f_j S_l$ through the cell face S_l we obtain the surface integral

$$\int_S f dS = \sum_l F_l = \sum_l \int_{S_l} f dS \approx \sum_l f_l S_l, \qquad l = w, e, s, n, b, t. \tag{A.1}$$

Approximation of volume integrals The integral source term Q_P in the subvolume P is calculated as the volume integral over the subvolume. Assuming the existence of a representing average value q_p at the cell center, we get

$$Q_P = \int_\Omega q d\Omega \approx q_P \triangle\Omega.$$

Discretization of the convective term The convective term of the general transport equation is approximated by

$$F_l^c = \int_{S_l} \Phi u_j \mathbf{n}_j dS_l \approx \dot{m}_l \Phi_l,$$

where $\dot{m}_l$ is the appropriate mass flow.

The flows of Φ have to be determined at the the cell faces. The equations are solved at the cell centers though. Therefore the flows must be interpolated from the cell centers at the cell faces. Such an interpolation method of first order is the *Upwind Differencing Scheme*

$$\Phi_e = \begin{cases} \Phi_E, & \text{if } (\mathbf{u} \cdot \mathbf{n}_l) < 0 \\ \Phi_P, & \text{if } (\mathbf{u} \cdot \mathbf{n}_l) > 0. \end{cases}$$

A method of second order is the *Central Differencing Scheme* which uses linear interpolation

$$\Phi_l = \lambda_l \Phi_L + (1 - \lambda_l)\Phi_p.$$

The interpolation factor will be determined by

$$\lambda_e = \frac{|\mathbf{r}_l - \mathbf{r}_P|}{|\mathbf{r}_L - \mathbf{r}_P|}.$$

The vectors $\mathbf{r}_l$ are the position vectors of the corresponding points.

Discretization of the diffusive term The diffusive term can be approximated by

$$F_l^d = \int_{S_l} \Gamma \frac{\partial \Phi}{\partial x_j} \mathbf{n}_j dS_l \approx (\Gamma \text{grad} \Phi \mathbf{n})_l S_l.$$

Both the diffusion coefficient and the gradient of Φ must be determined at the cell face, for example by linear interpolation. For this interpolation, gradients from cell centers have to be taken. A representing gradient at the cell center is obtained by averaging over the whole cell volume

$$\left(\frac{\partial \Phi}{\partial x_i} \right)_P \approx \frac{\int \frac{\partial \Phi}{\partial x_i} d\Omega}{\triangle \Omega}.$$

Again apply Gauß' divergence theorem and transform the volume integral into a surface integral

$$\begin{aligned} \int \frac{\partial \Phi}{\partial x_i} d\Omega = \int_S \Phi \mathbf{i}_i \mathbf{n} dS &\approx \sum \Phi_l S_l^i, \qquad l = e, n, w, s \ldots \\ \Rightarrow \left(\frac{\partial \Phi}{\partial x_i} \right)_P &\approx \frac{\sum_l \Phi_l S_l^i}{\triangle \Omega}. \end{aligned}$$

B Numerical methods for solving the hydrodynamic equations

Reynolds numbers of technical fluid flows, especially in turbo machinery are in the turbulent range. Basically turbulent flows can be computed by the following three models

- Direct Numerical Simulation
- Large Eddy Simulation
- Statistical description of the turbulence by means of the Reynolds-averaged Navier-Stokes equations.

Direct Numerical Simulation First of all we consider the Direct Numerical Simulation, which solves the original three-dimensional unsteady Navier-Stokes equations. To capture all scales of turbulence, even the smallest eddies have to be resolved by the discretization of time and space. Note that in fluid dynamics, eddies are generated by the swirling of a fluid. The essential number of grid points N of a computational mesh is supposed to be proportional to the third power of the Reynolds number, i.e.

$$N \sim Re^3.$$

As with technical fluid flows, where Reynolds numbers greater than 10^5 can appear, direct simulations are only possible against the background of enormous calculating capacity and calculating time.

Large Eddy Simulation The global flow field is influenced more or less by the big eddies, which carry most of the energy. The Large Eddy Simulation resolves the three-dimensional unsteady development of these eddies. The separation of the spatial scales is obtained by a low-pass filtering of the Navier-Stokes equations. The advantage of the LES is a certain economy of computational time, as the smallest spatial structures need not be resolved. A drawback is the calculation of flow near solid walls with high Reynolds numbers, as in those regions a near wall resolution similar to that of a DNS is necessary.

Statistical modeling of the turbulence By averaging the incompressible Navier-Stokes equations in time, a considerable simplification is achieved. The statistical consideration of the turbulence is due to the separation approach by Reynolds. Thus for stationary problems a local flow quantity Φ can be split into a temporal spatial average value $\bar{\Phi}$ and a fluctuation part Φ'

$$\Phi(x_i, t) = \bar{\Phi}(x_i) + \Phi'(x_i, t). \tag{B.1}$$

The temporal averaged quantity $\bar{\Phi}(x_i)$ is obtained by averaging over a time distance T, which is long enough

$$\bar{\Phi}(x_i) = \lim_{T\to\infty} \frac{1}{T} \int_t^{t+T} \Phi(x_i, t) dt. \tag{B.2}$$

For the temporal average of the fluctuation value we get

$$\bar{\Phi}'(x_i, t) = 0.$$

This derivation can also be applied to instationary flows, as long as the global temporal alteration of the fluid flow occurs on a slower scale than the turbulent fluctuations. The integration time T has to be large enough to compute a presentable average value, but small in contrast to the global time scale.

Inserting the separation ansatz presented in (B.1) in the Navier-Stokes equations and temporal averaging of the resulting equations results in the **Reynolds-averaged Navier-Stokes equations**

$$\frac{\partial \bar{u}_i}{\partial x_i} = 0, \tag{B.3}$$

$$\frac{\partial \bar{u}_i}{\partial t} + \bar{u}_j \frac{\partial \bar{u}_i}{\partial x_j} = -\frac{1}{\rho}\frac{\partial \bar{p}}{\partial x_i} + \frac{\partial}{\partial x_j}\left[\nu\left(\frac{\partial \bar{u}_i}{\partial x_j} + \frac{\partial \bar{u}_j}{\partial x_i}\right) - \overline{u_i' u_j'}\right]. \tag{B.4}$$

This system of equations describes the transport of the temporal averaged velocity and pressure in contrast to the original Navier-Stokes equations. It contains the additional Reynolds stress tensor $\overline{u_i' u_j'}$, which results from the averaging of the convective terms. The Reynolds stresses display the temporal averaged effect of the turbulent convection.

As the Reynolds stress tensor is unknown, the system of equations is primary not closed. This problem can be solved by introducing additional advection equations to describe the Reynolds stress tensor.

C Linearisation of the conservation equations for acoustics

The following section deals with the linearisation of the conservation of mass and conservation of momentum equations in order to obtain the acoustic equations for the EIF method. The derivations will be done in two dimensions for simplification purposes. First we consider the continuity equation in 2D, which reads

$$\frac{\partial \rho}{\partial t} + \frac{\partial}{\partial x}(\rho u) + \frac{\partial}{\partial y}(\rho v) = 0, \tag{C.1}$$

$$\Leftrightarrow \frac{\partial \rho}{\partial t} + \rho\left(\frac{\partial u}{\partial x} + \frac{\partial v}{\partial y}\right) + u\frac{\partial \rho}{\partial x} + v\frac{\partial \rho}{\partial y} = 0, \tag{C.2}$$

with the corresponding perturbation ansatz

$$\begin{aligned} u &= U + u', \\ v &= V + v', \\ \rho &= \rho_0 + \rho'. \end{aligned}$$

Remember that

$$\begin{aligned} f_u &= (\rho_0 + \rho') \cdot u' + U \cdot \rho', \\ f_v &= (\rho_0 + \rho') \cdot v' + V \cdot \rho'. \end{aligned}$$

Equation (C.1) can be transformed to

$$\frac{\partial \rho_0}{\partial t} + \frac{\partial \rho'}{\partial t} + \frac{\partial}{\partial x}\left(u' \cdot (\rho_0 + \rho') + U \cdot \rho_0 + U \cdot \rho'\right) + \frac{\partial}{\partial y}\left(v' \cdot (\rho_0 + \rho') + V \cdot \rho_0 + V \cdot \rho'\right) = 0$$

$$\Leftrightarrow \quad \underbrace{\frac{\partial \rho_0}{\partial t} + \frac{\partial}{\partial x}\Big(\rho_0 \cdot U\Big) + \frac{\partial}{\partial y}\Big(\rho_0 \cdot V\Big)}_{\equiv 0} +$$

$$+ \quad \frac{\partial \rho'}{\partial t} + \frac{\partial}{\partial x}\left(\underbrace{u' \cdot (\rho_0 + \rho') + U \cdot \rho'}_{=f_u}\right) + \frac{\partial}{\partial y}\left(\underbrace{v' \cdot (\rho_0 + \rho') + V \cdot \rho'}_{=f_v}\right) = 0.$$

as result we get the linearised continuity equation for compressible fluids in 2D

$$\frac{\partial \rho'}{\partial t} + \frac{\partial f_u}{\partial x} + \frac{\partial f_v}{\partial y} = 0. \tag{C.3}$$

Next, the Euler equations in 2D will be linearised

$$\frac{\partial}{\partial t}(\rho u) + \frac{\partial}{\partial x}(\rho u^2 + p) + \frac{\partial}{\partial y}(\rho uv) = 0, \tag{C.4}$$

$$\frac{\partial}{\partial t}(\rho v) + \frac{\partial}{\partial x}(\rho uv) + \frac{\partial}{\partial y}(\rho v^2 + p) = 0. \tag{C.5}$$

Again we use the perturbation ansatz as given above and in addition

$$p = P + p'. \tag{C.6}$$

The derivation of the acoustic equations shall be considered separated, that is first for the x-coordinate and secondly for the y-coordinate: Therefore

$$\begin{aligned} \frac{\partial}{\partial t}\Big[(\rho_0 + \rho')(U + u')\Big] &+ \frac{\partial}{\partial x}\Big[(\rho_0 + \rho')(U + u')^2 + (P + p')\Big] \\ &+ \frac{\partial}{\partial y}\Big[(\rho_0 + \rho')(U + u')(V + v')\Big] = 0. \end{aligned}$$

Various transformations give the following intermediate expression

$$\begin{aligned} \frac{\partial}{\partial t}\Big(\rho_0 \cdot U + f_u\Big) + \frac{\partial}{\partial x}\Bigg((U + u') \cdot \Big[\underbrace{u'(\rho_0 + \rho') + U\rho'}_{=f_u} + U\rho_0\Big] + (P + p')\Bigg) &+ \\ \frac{\partial}{\partial y}\Bigg((V + v') \cdot \Big[\underbrace{u'(\rho_0 + \rho') + U\rho'}_{=f_u} + U\rho_0\Big]\Bigg) &= 0, \end{aligned}$$

which results in the final acoustic equation for the first coordinate x

$$\begin{aligned} \underbrace{\frac{\partial}{\partial t}(\rho_0 U) + \frac{\partial}{\partial x}\Big(\rho_0 U^2 + p'\Big) + \frac{\partial}{\partial y}\Big(\rho_0 UV\Big)}_{\equiv 0} &+ \\ \frac{\partial}{\partial t}(f_u) + \frac{\partial}{\partial x}\Big((U + u') \cdot f_u + \rho_0 U u' + p'\Big) & \\ \frac{\partial}{\partial y}\Big((V + v') \cdot f_u + \rho_0 U v'\Big) &= 0. \end{aligned}$$

The same derivation is pursued for the y-coordinate. At the end we receive a two-dimensional system of differential equations for the acoustic field

$$\frac{\partial f_u}{\partial t} + \frac{\partial}{\partial x}\Big(f_u \cdot (U + u') + \rho_0 U u' + p'\Big) + \frac{\partial}{\partial y}\Big(f_u \cdot (V + v') + \rho_0 U v'\Big) = 0, \tag{C.7}$$

$$\frac{\partial f_v}{\partial t} + \frac{\partial}{\partial x}\Big(f_v \cdot (U + u') + \rho_0 V u'\Big) + \frac{\partial}{\partial y}\Big(f_v \cdot (V + v') + \rho_0 V v' + p'\Big) = 0. \tag{C.8}$$

The analog system of equations for the acoustic in 3D reads

$$
\begin{array}{lllllllll}
\frac{\partial \rho'}{\partial t} & + & \frac{\partial}{\partial x}\Big(f_u\Big) & + & \frac{\partial}{\partial y}\Big(f_v\Big) & + & \frac{\partial}{\partial z}\Big(f_w\Big) & = 0, \\
\frac{\partial f_u}{\partial t} & + & \frac{\partial}{\partial x}\Big(f_u u + \rho_0 U u' + p'\Big) & + & \frac{\partial}{\partial y}\Big(f_u v + \rho_0 U v'\Big) & + & \frac{\partial}{\partial z}\Big(f_u w + \rho_0 U w'\Big) & = 0, \\
\frac{\partial f_v}{\partial t} & + & \frac{\partial}{\partial x}\Big(f_v u + \rho_0 V u'\Big) & + & \frac{\partial}{\partial y}\Big(f_v v + \rho_0 V v' + p'\Big) & + & \frac{\partial}{\partial z}\Big(f_v w + \rho_0 V w'\Big) & = 0, \\
\frac{\partial f_w}{\partial t} & + & \frac{\partial}{\partial x}\Big(f_w u + \rho_0 W u'\Big) & + & \frac{\partial}{\partial y}\Big(f_w v + \rho_0 W v'\Big) & + & \frac{\partial}{\partial z}\Big(f_w w + \rho_0 W w' + p'\Big) & = 0.
\end{array}
$$

The equivalent equations in subscript notation read

$$
\begin{array}{lllll}
\frac{\partial \rho}{\partial t} & + & \frac{\partial}{\partial x_i}\Big(f_i\Big) & = 0, \\
\frac{\partial \rho}{\partial t} & + & \frac{\partial}{\partial x_j}\Big(f_i \cdot (U_j + u'_j) + \rho_0 \cdot U_i \cdot u'_j + p' \cdot \delta_{ij}\Big) & = 0.
\end{array}
$$

For numerical purposes we take the following equation into account

$$
\left.\frac{\partial p}{\partial \rho}\right|_S = a_s^2 \Rightarrow \frac{\frac{\partial p}{\partial t}}{\frac{\partial \rho}{\partial t}} = a_s^2 \Rightarrow \frac{\partial \rho}{\partial t} = \frac{1}{a_s^2}\frac{\partial p}{\partial t} \tag{C.9}
$$

$$
\text{and} \qquad \frac{\partial \rho}{\partial x} = \frac{1}{a_s^2}\frac{\partial p}{\partial x} \tag{C.10}
$$

$$
\frac{\partial \rho}{\partial y} = \frac{1}{a_s^2}\frac{\partial p}{\partial y}. \tag{C.11}
$$

Equation (C.2) can be transformed to

$$
\begin{aligned}
\frac{1}{a_s^2}\frac{\partial p}{\partial t} + \frac{1}{a_s^2}u\frac{\partial p}{\partial x} + \frac{1}{a_s^2}v\frac{\partial p}{\partial y} + \rho\left(\frac{\partial u}{\partial x} + \frac{\partial v}{\partial y}\right) &= 0, \\
\Leftrightarrow \frac{\partial p}{\partial t} + u\frac{\partial p}{\partial x} + v\frac{\partial p}{\partial y} + a_s^2 \cdot \rho\left(\frac{\partial u}{\partial x} + \frac{\partial v}{\partial y}\right) &= 0. \qquad \text{(C.12)}
\end{aligned}
$$

The second equation (C.12) is called the 2nd form of the continuity equation. By using (C.6) the continuity equation in its second form can be linearised to either one equation dependent of the pressure fluctuation p', and with the aid of (C.9) till (C.11) to one equation dependent of ρ'

$$
\begin{aligned}
\frac{\partial p'}{\partial t} + u \cdot \frac{\partial p'}{\partial x} + v \cdot \frac{\partial p'}{\partial y} + a_s^2 \rho\left[\frac{\partial u'}{\partial x} + \frac{\partial v'}{\partial y}\right] &= -\left(\frac{\partial P}{\partial t} + u \cdot \frac{\partial P}{\partial x} + v \cdot \frac{\partial P}{\partial v} + a_s^2 \cdot \rho\left[\frac{\partial U}{\partial x} + \frac{\partial V}{\partial y}\right]\right), \\
\frac{\partial \rho'}{\partial t} + u \cdot \frac{\partial \rho'}{\partial x} + v \cdot \frac{\partial \rho'}{\partial y} + \rho\left[\frac{\partial u'}{\partial x} + \frac{\partial v'}{\partial y}\right] &= -\left(\frac{\partial \rho_0}{\partial t} + u \cdot \frac{\partial \rho_0}{\partial x} + v \cdot \frac{\partial \rho_0}{\partial y} + \rho\left[\frac{\partial U}{\partial x} + \frac{\partial V}{\partial y}\right]\right).
\end{aligned}
$$

Under the assumption that

$$
\begin{aligned}
u'_i &\ll U_i \\
\rho' &\ll \rho_0 \\
p' &\ll P,
\end{aligned}
$$

the acoustic fluctuation quantities p' and ρ' respectively are yielded by the following system of equations

$$\begin{aligned}
\frac{\partial p'}{\partial t} + U\frac{\partial p'}{\partial x} + V\frac{\partial p'}{\partial y} + a_s^2\rho_0\left[\frac{\partial u'}{\partial x} + \frac{\partial v'}{\partial y}\right] &= -\left(\frac{\partial P}{\partial t} + U\frac{\partial P}{\partial x} + V\frac{\partial P}{\partial v} + a_s^2\rho_0\left[\frac{\partial U}{\partial x} + \frac{\partial V}{\partial y}\right]\right), \\
\frac{\partial \rho'}{\partial t} + U\frac{\partial \rho'}{\partial x} + V\frac{\partial \rho'}{\partial y} + \rho_0\left[\frac{\partial u'}{\partial x} + \frac{\partial v'}{\partial y}\right] &= -\left(\frac{\partial \rho_0}{\partial t} + U\frac{\partial \rho_0}{\partial x} + V\frac{\partial \rho_0}{\partial y} + \rho_0\left[\frac{\partial U}{\partial x} + \frac{\partial V}{\partial y}\right]\right).
\end{aligned}$$

The right hand side contains quantities that can be computed by a preceding calculation of the URANS equations or by a foregoing LES.

References

[Hardin&Pope94] Hardin J.C., Pope D.S., *An Acoustic/Viscous Splitting Technique for Computational Aeroacoustics*, Theoret. Comput. Fluid Dynamics Vol. 6, pp. 323-340, 1994,

[Lighthill52] Lighthill M.J., *On sound generated aerodynamically Part I. General Theory*, Proceedings of the Royal Society of London. Series A, Mathematical and Physical Sciences Vol. 211, No. 1107, pp. 564-587, 1952,

[Shen&Sørensen99a] Shen W.Z., Sørensen J.N., *Aeroacoustic Modelling of Low-Speed Flows*, Theorte. Comput. Fluid Dynamics, Vol. 13, pp. 271-289, 1999

[Shen&Sørensen99b] Shen W.Z., Sørensen J.N., *Comment on the Aeroacoustic Formulation of Hardin and Pope*, AIAA Journal Vol. 37, No. 1, 1999,

[Tam&Webb93] Tam C.K., Webb J.C., *Dispersion-relation-preserving schemes for computational aeroacoustics*, J. Computat. Phys., Vol. 107, No. 2, pp. 262-281, 1993,